AIAA SciTech Forum
8–12 January 2018, Kissimmee, Florida
2018 AIAA Guidance, Navigation, and Control Conference

10.2514/6.2018-1857

Decentralized Conflict Detection and Resolution Using Intent-Based Probabilistic Trajectory Prediction

Nobuhiro Yokoyama[1]
National Defense Academy, Kanagawa, 239-8686, Japan

This paper proposes a decentralized conflict detection and resolution method using probabilistic trajectory prediction combined with intent inference. In our method, by incorporating the results of inverse optimal control for intent inference and the unscented transform for predicting nonlinear probabilistic state propagation, conflict detection and resolution problem is formulated as a decentralized model predictive control (MPC) problem. The method can cover linear/nonlinear uncertain behaviors of aircraft due to the wind effect, the deviation of navigation and control strategy, and the inaccuracy of inferred intent. In addition, it can circumvent nonconvex constraints representing the separation condition as well as flight performance limits in computationally tractable way by decoupling and convexification technique. Through numerical simulations, the effectiveness of the method is demonstrated in terms of the validity of the obtained conflict-free trajectories and the computational efficiency.

I. Introduction

Current trend of increase in air traffic volume necessitates the modernization of communication, surveillance, navigation (CNS) and air traffic management (ATM) system using advanced technologies. To meet those requirements, new operation programs called as NextGen[1], SESAR[2], and CARATS[3], have been initiated by the U.S., Europe, and Japan, respectively. In these programs, active research and development have been conducted to improve the operational flexibility by allowing the change of trajectories according to the situation and by partly delegating the responsibility of maintaining separation to individual aircraft. Thus, decentralized separation assurance, or self-separation, has been regarded as one of the key technologies to enable this kind of advanced operations. With this in mind, the objective of this study is to propose a new method for decentralized conflict detection and resolution to achieve self-separation.

In general, conflict detection involves the prediction of future trajectories of neighboring aircraft based on the observation and/or estimation of the current state of them, where Automatic Dependent Surveillance Broadcast (ADS-B)[4] is currently becoming an available technology for this purpose. Moreover, it has been conceived in some future operational concepts to utilize ADS-B for broadcasting four-dimensional flight plans[5,6] such as the sequence of waypoints' locations and corresponding times to pass through them. With this technology, it is expected that more accurate prediction of future trajectories is enabled. Nevertheless, even if the flight plan information of the neighboring aircraft is available, it is still necessary to monitor the conformance to it[7]. Then, if the conformance is not good, it is also necessary to infer the other possible intent hiding behind the current trajectory[8-12]. This is because the aircraft may not necessarily conform to the flight plan due to tactical reasons such as to attain conflict resolution with the neighboring aircraft and to avoid adverse weather areas or special use airspace. Therefore, the conflict detection and resolution method in this study adopts the trajectory prediction combined with the intent inference method, which we developed in our previous work[12].

Although a lot of trajectory prediction methods have been proposed so far, they can be categorized to nominal, worst-case, and probabilistic ones[13]. The nominal methods project the current state of the aircraft along a single trajectory with or without consideration of validated/inferred flight intent. It is simple but cannot support the uncertain elements of the aircraft behavior[14] such as the potential change of the tactical intent, the navigation strategy and the control law adopted therein, the effect of wind, and so on. The worst-case methods are the other

[1] Associate Professor, Department of Aerospace Engineering, 1-10-20 Hashirimizu, Yokosuka, AIAA Senior Member.

extreme of modeling. They generate a set of any possible trajectories subject to the uncertainty. The probabilistic methods can also calculate the set of any possible trajectories, but it can associate the probability densify function (PDF) with it as well[15]. Thus, as pointed out in Ref. 13, the nominal and the worst-case methods can be interpreted as the special case of the probabilistic ones. Refs 16 and 17 proposed methods to predict the probabilistic state propagation following the verified/inferred intent. Using a simplified integration technique of the PDFs, the methods attain reasonable conflict detection and/or resolution. However, the method does not support the nonlinear dynamics, which naturally arise in the non-holonomic behavior of the aircraft kinematics and in the navigation strategies used therein. Ref. 18 also presented a probabilistic trajectory prediction method for conflict resolution considering the wind uncertainty. Their method covers the uncertain nonlinear dynamics by utilizing the generalized polynomial chaos expansion[19], and it solves the chance-constrained model predictive control (MPC) problem for conflict resolution. However, the intent information is not explicitly handled.

On the other hand, the method proposed in this paper calculates the state propagation of the nonlinear dynamic system using an intent-based trajectory prediction combined with the unscented transform[20-22]. The unscented transform is a simple but powerful tool to calculate nonlinear behaviors of stochastic systems. Originally, it was proposed within the framework of nonlinear Kalman filters[20, 21], but it has also been applied to the prediction-based control of stochastic dynamical systems[22]. In our method, we apply the unscented transform to cover the linear/nonlinear uncertain behaviors due to the wind effect, the navigation/control strategy, and the inaccuracy of inferred intent.

As pointed out in Ref. 13, there is an interdependence between conflict detection and conflict resolution. Thus, in our framework, conflict detection and resolution problems are simultaneously formulated as a decentralized MPC problem to resolve the potential conflict with the set of uncertain trajectories. The decentralized computations of individual MPCs are assured by a coordination term in the objective function and compatibility constraints for separation, both of which reflects the inferred intent. Moreover, the inherent nonconvexities in separation constraints as well as those of flight performance limits are circumvent by sequential convexification approach[23] for computational tractability. Thus, the MPC problem is formulated as a convex quadratically constrained quadratic program (convex-QCQP)[23]. Together with the intent inference problem, which is also formulated as a convex QP, our method can be executed in real-time with convergence guarantee.

Through numerical simulations, the effectiveness of the developed algorithm is confirmed in terms of the computational efficiency and the validity of calculated trajectories/predictions.

II. Conflict Detection and Resolution Using Intent-Based Trajectory Prediction

A. Motion Model

For simplicity, we assume that the motion of an aircraft is constrained on the horizontal plane. The state equations of the aircraft is written as follows:

$$\begin{bmatrix} \dot{x} \\ \dot{y} \\ \dot{\psi} \\ \dot{V} \end{bmatrix} = \begin{bmatrix} V\cos\psi + w_x \\ V\sin\psi + w_y \\ (g/V)\tan\varphi \\ a \end{bmatrix} \tag{1}$$

where (x, y) is the position of the aircraft in the horizontal coordinate system, V is the magnitude of the airspeed, w_x and w_y are the wind velocity in the x- and y-directions, respectively, ψ is the heading angle, g is the gravitational acceleration, φ is the bank angle, and a is the axial acceleration.

B. Intent-Based Probabilistic Trajectory Prediction Using Unscented Transform

Let us assume that the time history of the state of the "target" neighboring aircraft and its flight plan is available via ADS-B, and further assume that the time history of the state is the approximate local optimum for certain operational objectives of the target aircraft. The intent inference method adopted in this study solves the inverse optimal control problem, i.e., it calculates the weight of each term of the objective function that represents the flight intent. By incorporating the second-order optimality condition, i.e., the positive definiteness of the projected Hessian of the Lagrangian, the method accounts for both the necessity and sufficiency of the approximate local optimality of

the given trajectory. Moreover, the method also guarantees the uniqueness of the inferred intent. We summarize the method in Appendix. Further details are available in Ref. 12.

Based on the inferred intent, our method predicts the probabilistic state propagation of the target aircraft. In our method for trajectory prediction, Eq. (1) is discretized by the zeroth order hold. Hereafter, variables with the subscript k denote those at time $t = k\Delta t$, where Δt is the time step length. We assume that the probabilistic state propagation is caused by the uncertainties of i) the wind effect, ii) the navigation/control strategy of the target aircraft and its associated error, and iii) the error or the potential change of the desirable velocity vector associated with the flight intent. A nonlinear discrete time system involving the above uncertain elements is given as follows: Let $\boldsymbol{y}_k$ be an augmented state of the system defined as

$$\boldsymbol{y}_k := [\, x_k \;\; y_k \;\; \psi_k \;\; V_k \;\; a_k \;\; u_{dk} \;\; v_{dk} \,]^T$$

where $[\, u_{dk} \;\; v_{dk} \,]^T$ denotes the desirable ground velocity vector associated with the inferred intent. The state equation of the augmented system is then represented as

$$\boldsymbol{y}_{k+1} = \tilde{\boldsymbol{f}}(\boldsymbol{y}_k, p, w_{ak}) + \boldsymbol{q}_k \Delta t \tag{2}$$

$$\tilde{\boldsymbol{f}}(\boldsymbol{y}_k, \delta\tau_k, \delta a_k) := \begin{bmatrix} x_k + (V_k \cos\psi_k + \bar{w}_{xk})\Delta t \\ y_k + (V_k \sin\psi_k + \bar{w}_{yk})\Delta t \\ \psi_k + (g\Delta t / V_k)\tan[\mathrm{sat}(\hat{\varphi}_k \mid -\varphi_{\max}, \varphi_{\max})] \\ V_k + a_k \Delta t \\ \mathrm{sat}(a_k + \delta a_k \Delta t \mid \hat{a}_{\min}, \hat{a}_{\max}) \\ u_{dk} \\ v_{dk} \end{bmatrix}, \quad \boldsymbol{q}_k := \begin{bmatrix} \delta w_{xk} \\ \delta w_{yk} \\ \delta\omega_k \\ 0 \\ 0 \\ \delta u_{dk} \\ \delta v_{dk} \end{bmatrix}, \tag{3}$$

$$\hat{\varphi}_k = \tan^{-1}\left[\frac{V_k}{g\,\hat{\tau}c^{\delta\tau_k}}\left\{\tan^{-1}\left(\frac{v_{dk} - \bar{w}_{yk}}{u_{dk} - \bar{w}_{xk}}\right) - \psi_k\right\}\right] \tag{4}$$

where $\hat{\tau}$ and c are constants, $\delta\tau_k$ denotes an uncertain parameter to account for the deviation of the navigation time constant which is represented by $\hat{\tau}c^{\delta\tau_k}$, $\hat{a}_{\min}$ and $\hat{a}_{\max}$ denote the assumed values of the minimum and the maximum acceleration, respectively, $\delta\omega_k$ and δa_k denote the stochastic variables accounting for the errors/deviations of navigation/control, $(\delta u_{dk}, \delta v_{dk})$ denotes the generator of the random walk of the desirable velocity vector, and the function $\mathrm{sat}(x \mid x_L, x_U)$ is defined as

$$\mathrm{sat}(x \mid x_L, x_U) := \begin{cases} x_L & : \text{if } x < x_L \\ x & : \text{if } x_L \le x \le x_U \\ x_U & : \text{if } x_U < x \end{cases} \tag{5}$$

Note that the navigation/control strategy is approximated by an uncertain first-order lag system for simplicity, i.e., if $-\varphi_{\max} \le \hat{\varphi}_k \le \varphi_{\max}$, substituting Eq. (4) into the third row of Eq. (2) yields the following first-order lag system:

$$\psi_{k+1} = \psi_k + \frac{\Delta t}{\hat{\tau}c^{\delta\tau_k}}\left\{\tan^{-1}\left(\frac{v_{dk} - \bar{w}_{yk}}{u_{dk} - \bar{w}_{xk}}\right) - \psi_k\right\} \tag{6}$$

The stochastic variables appearing in Eq. (2) covers the above-mentioned uncertainties i) - iii), and they are assumed to yield the following Gaussian distributions:

$$\begin{bmatrix} \delta w_{xk} \\ \delta w_{yk} \end{bmatrix} \sim N\left(\begin{bmatrix} 0 \\ 0 \end{bmatrix}, \begin{bmatrix} {\sigma_{wx}}^2 & 0 \\ 0 & {\sigma_{wy}}^2 \end{bmatrix}\right),$$

$$\delta\omega_k \sim N(0, {\sigma_\omega}^2),$$

$$\delta a_k \sim N(0, {\sigma_a}^2),$$

$$\delta\tau_k \sim N(0, {\sigma_\tau}^2),$$

$$\begin{bmatrix} \delta u_{dk} \\ \delta v_{dk} \end{bmatrix} \sim N\left(\begin{bmatrix} 0 \\ 0 \end{bmatrix}, \begin{bmatrix} {\sigma_{ud}}^2 & 0 \\ 0 & {\sigma_{vd}}^2 \end{bmatrix}\right)$$

Now, let the mean and the covariance of $\boldsymbol{y}_k$ predicted at $t = N\Delta t$ $(N \in \mathbb{N})$ be $\boldsymbol{m}_{k|N} \in \mathbb{R}^7$ and $\boldsymbol{P}_{k|N} \in \mathbb{R}^{7\times 7}$, respectively. The propagation of these probabilistic parameters can then be obtained by the unscented transform as

follows: Let n denote the sum of the dimensions of $[\boldsymbol{y}_k{}^T \quad \delta\tau_k \quad \delta a_k]^T$, i.e., $n=9$. Calculate the following $(2n+1)$ sigma-points $\boldsymbol{s}_{k|N}^{(0)}, \boldsymbol{s}_{k|N}^{(1)}, \cdots, \boldsymbol{s}_{k|N}^{(2n)} \in \mathbb{R}^n$ by

$$\begin{aligned}
\boldsymbol{s}_{k|N}^{(0)} &= \tilde{\boldsymbol{m}}_{k|N} \\
\boldsymbol{s}_{k|N}^{(i)} &= \tilde{\boldsymbol{m}}_{k|N} + \left[\sqrt{(n+\alpha)\tilde{\boldsymbol{P}}_{k|N}}\right]_i, \quad i=1,\cdots,n \\
\boldsymbol{s}_{k|N}^{(i)} &= \tilde{\boldsymbol{m}}_{k|N} - \left[\sqrt{(n+\alpha)\tilde{\boldsymbol{P}}_{k|N}}\right]_{i-n}, \quad i=n+1,\cdots,2n
\end{aligned} \tag{7}$$

where $\tilde{\boldsymbol{m}}_{k|N}$ and $\tilde{\boldsymbol{P}}_{k|N}$ are defined as

$$\tilde{\boldsymbol{m}}_{k|N} = \begin{bmatrix} \boldsymbol{m}_{k|N} \\ \boldsymbol{0}_{2\times 1} \end{bmatrix}, \quad \tilde{\boldsymbol{P}}_{k|N} = \mathrm{diag}(\boldsymbol{P}_{k|N}, {\sigma_\tau}^2, {\sigma_a}^2) \tag{8}$$

and α is a tuning parameter. The mean and the covariance of $\boldsymbol{y}_{k+1}$ predicted at $t=N\Delta t$, i.e., $\boldsymbol{m}_{k+1|N}$ and $\boldsymbol{P}_{k+1|N}$, can then be obtained by the following equations

$$\boldsymbol{m}_{k+1|N} = \sum_{i=0}^{2n} W_i^{(m)} \tilde{\boldsymbol{f}}(\boldsymbol{s}_{k|N}^{(i)}) \tag{9}$$

$$\boldsymbol{P}_{k+1|N} = \sum_{i=0}^{2n} W_i^{(c)} [\tilde{\boldsymbol{f}}(\boldsymbol{s}_{k|N}^{(i)}) - \boldsymbol{m}_{k+1|N}][\tilde{\boldsymbol{f}}(\boldsymbol{s}_{k|N}^{(i)}) - \boldsymbol{m}_{k+1|N}]^T + \Delta t^2\, \mathrm{diag}(\sigma_{wx}, \sigma_{yx}, \sigma_\omega, 0, 0, \sigma_{ud}, \sigma_{vd})^2 \tag{10}$$

where $W_i^{(m)}, W_i^{(c)}, i=0,1,\cdots,2n$ are weighting coefficients. Equations (7)-(10) constitutes a cycle of the unscented transform, and we can obtain the sequence of $\{\boldsymbol{m}_{k|N}\}$ and $\{\boldsymbol{P}_{k|N}\}$, $k=N+1, N+2, \cdots$ by repeating this cycle. The advantage of the unscented transform is its simplicity while it can accurately capture the first- and second-order moments of the distribution[20, 21]. In our method, the mean $\boldsymbol{y}_{N|N}$ is obtained by concatenating the measured/estimated values of x_N, y_N, ψ_N, V_N, and a_N as well as the inferred values of u_{dN} and v_{dN} (see Appendix for the way to obtain these). The covariance $\boldsymbol{P}_{N|N}$, on the other hand, is given *a priori*.

Using the probabilistic parameters obtained by the above approach, the set of probable position of the target aircraft at time $t=k\Delta t$, i.e., $[x_k \quad y_k]^T$, is represented by

$$E(\hat{x}_{k|N}, \hat{y}_{k|N}, \boldsymbol{P}_{\mathrm{pos},k|N}, \mu) := \left\{ \begin{bmatrix} x_k \\ y_k \end{bmatrix} \in \mathbb{R}^2 \;\middle|\; \begin{bmatrix} x_k - \hat{x}_{k|N} \\ y_k - \hat{y}_{k|N} \end{bmatrix}^T \boldsymbol{P}_{\mathrm{pos},k|N}{}^{-1} \begin{bmatrix} x_k - \hat{x}_{k|N} \\ y_k - \hat{y}_{k|N} \end{bmatrix} \le \mu^2 \right\} \tag{11}$$

where $[\hat{x}_{k|N} \quad \hat{y}_{k|N}]^T \in \mathbb{R}^2$ and $\boldsymbol{P}_{\mathrm{pos},k|N} \in \mathbb{R}^{2\times 2}$ denote the mean and the covariance of $[x_k \quad y_k]^T$, and μ denotes the degree of uncertainty which is given *a priori*. Note that $[\hat{x}_{k|N} \quad \hat{y}_{k|N}]^T$ and $\boldsymbol{P}_{\mathrm{pos},k|N}$ are the subvector of $\boldsymbol{m}_{k|N}$ and submatrix of $\boldsymbol{P}_{k|N}$, respectively.

C. Decentralized MPC for Conflict Detection and Resolution

Given the set of possible trajectories of the neighboring aircraft in the form of Eq. (11), our method solves an MPC problem for conflict detection and resolution by calculating the optimal control input of the own aircraft.

Let us assume that the own aircraft's motion is constrained by the following performance constraints.

$$V_{\min} \le V \le V_{\max} \tag{12}$$

$$-\varphi_{\max} \le \varphi \le \varphi_{\max} \tag{13}$$

$$a_{\min} \le a \le a_{\max} \tag{14}$$

where $0 < V_{\min}$ and $a_{\min} < 0 < a_{\max}$ holds. By introducing the following additional variables:

$$\begin{aligned}
u &:= V\cos\psi + w_x \\
v &:= V\sin\psi + w_y \\
\omega &:= g\tan\varphi / V \\
\xi &:= a / V
\end{aligned}$$

Eq. (1) can be rewritten as the following system

$$\begin{bmatrix} \dot{x} \\ \dot{y} \\ \dot{u} \\ \dot{v} \end{bmatrix} = \begin{bmatrix} u \\ v \\ -(v-w_y)\omega + (u-w_x)\xi \\ (u-w_x)\omega + (v-w_y)\xi \end{bmatrix} \tag{15}$$

Similarly to the trajectory prediction, we discretize the original continuous-time system to the discrete-time system. By applying the zeroth-order hold to Eq. (15) and assuming that w_x and w_y are constant values $w_{x|N}$ and $w_{y|N}$, respectively, during the prediction in MPC at $t = N\Delta t$, we obtain

$$\begin{bmatrix} x_{k+1|N} \\ y_{k+1|N} \\ u_{k+1|N} \\ v_{k+1|N} \end{bmatrix} = \begin{bmatrix} x_{k|N} + u_{k|N}\Delta t \\ y_{k|N} + v_{k|N}\Delta t \\ u_{k|N} + [-(v_{k|N} - w_{y|N})\omega_{k|N} + (u_{k|N} - w_{x|N})\xi_{k|N}]\Delta t \\ v_{k|N} + [(u_{k|N} - w_{x|N})\omega_{k|N} + (v_{k|N} - w_{y|N})\xi_{k|N}]\Delta t \end{bmatrix} \tag{16}$$

The performance constraints defined by Eqs. (12)-(14) can also be rewritten as

$$V_{\min}{}^2 \le (u_{k|N} - w_{x|N})^2 + (v_{k|N} - w_{y|N})^2 \le V_{\max}{}^2 \tag{17}$$

$$-g\tan\varphi_{\max} \le \omega_{k|N}\sqrt{(u_{k|N} - w_{x|N})^2 + (v_{k|N} - w_{y|N})^2} \le g\tan\varphi_{\max} \tag{18}$$

$$a_{\min} \le \xi_{k|N}\sqrt{(u_{k|N} - w_{x|N})^2 + (v_{k|N} - w_{y|N})^2} \le a_{\max} \tag{19}$$

Furthermore, by considering the trajectory uncertainty as in Eq. (11), the constraint for separation from j-th neighboring aircraft $(j = 1,\cdots,M)$ at time $t = k\Delta t$ can be represented by the following equation

$$\left\| \begin{bmatrix} x_{k|N} - x \\ y_{k|N} - y \end{bmatrix} \right\| \ge R, \quad \text{for } \forall \begin{bmatrix} x \\ y \end{bmatrix} \in E(\hat{x}_{k|N}^{(j)}, \hat{y}_{k|N}^{(j)}, \boldsymbol{P}_{\text{pos},k|N}^{(j)}, \mu) \tag{20}$$

where the superscript (j) denotes the variables of j-th neighboring aircraft $(j = 1,\cdots,M)$.

Let $t = (N + N_p)\Delta t \quad (N_p \in \mathbb{N} \setminus \{0\})$ be the horizon time of the MPC. We can now state the discrete-time optimal control problem defined over the finite time horizon $[N\Delta t, (N + N_p)\Delta t]$, as follows:

$$\begin{aligned} \text{minimize}: \quad & J := \sum_{k=N+1}^{N+N_p} [\bar{\rho}_1\{(x_{k|N} - x_{rk})^2 + (y_{k|N} - y_{rk})^2\} + \bar{\rho}_2\{(x_{k|N} - \hat{x}_{k|N}^{(0)})^2 + (y_{k|N} - \hat{y}_{k|N}^{(0)})^2\}] \\ & + \sum_{k=N}^{N+N_p-1} \bar{\rho}_3(\omega_{k|N}{}^2 + \xi_{k|N}{}^2) \end{aligned} \tag{21}$$

$$\text{subject to}: \quad [x_{N|N} \;\; y_{N|N} \;\; u_{N|N} \;\; v_{N|N}]^T = [x_N \;\; y_N \;\; u_N \;\; v_N]^T \tag{22}$$

Eq. (16), $k = N,\cdots,N+N_p-1$,
Eq. (17), $k = N+1,\cdots,N+N_p$,
Eqs. (18) and (19), $k = N,\cdots,N+N_p-1$, and
Eq. (20), $k = N+1,\cdots,N+N_p$, $j = 1,\cdots,M$

decision variables: $[x_{k|N} \;\; y_{k|N} \;\; u_{k|N} \;\; v_{k|N}]^T$, $k = N,\cdots,N+N_p$, $[\omega_{k|N} \;\; \xi_{k|N}]^T$, $k = N,\cdots,N+N_p-1$,

where $\bar{\rho}_1, \bar{\rho}_2$ and $\bar{\rho}_3$ are weighting parameters, $[x_{rk} \;\; y_{rk}]^T, k = 0,1,2,\cdots,$ are the points on the own aircraft's reference path which is expressed as the piecewise-linear interpolation of the sequence of designated waypoints and times to pass them, and $[\hat{x}_{k|N}^{(0)} \;\; \hat{y}_{k|N}^{(0)}]^T, k = N, N+1,\cdots,$ are the mean of the own aircraft's probabilistic position at $t = k\Delta t$ which is to be predicted by each of the neighboring aircraft at $t = N\Delta t$. We assume that the own aircraft also calculates its probabilistic trajectory and it is the same as those predicted by the neighboring aircraft. It should be noted that the inclusion of the term to track $[\hat{x}_{k|N}^{(0)} \;\; \hat{y}_{k|N}^{(0)}]^T, k = N, N+1,\cdots,$ has an effect that what the own aircraft plans to do well matches what the neighboring aircraft infer the own aircraft will do. In this way, we can expect the coordinated maneuver in conflict resolution.

Since Eqs. (16)-(20) are nonconvex, it is hard to guarantee the real-time convergence of the above MPC. Thus, for computational tractability, Eqs. (16)-(19) are convexified as follows:

$$\begin{bmatrix} x_{k+1|N} \\ y_{k+1|N} \\ u_{k+1|N} \\ v_{k+1|N} \end{bmatrix} = \begin{bmatrix} x_{k|N} + u_{k|N}\Delta t \\ y_{k|N} + v_{k|N}\Delta t \\ u_{k|N} + [(\overline{v}_{k|N} - w_{y|N})\overline{\omega}_{k|N} - (\overline{u}_{k|N} - w_{x|N})\overline{\xi}_{k|N} - (v_{k|N} - w_{y|N})\overline{\omega}_{k|N} \\ +(u_{k|N} - w_{x|N})\overline{\xi}_{k|N} - (\overline{v}_{k|N} - w_{y|N})\omega_{k|N} + (\overline{u}_{k|N} - w_{x|N})\xi_{k|N}]\Delta t \\ v_{k|N} + [-(\overline{u}_{k|N} - w_{x|N})\overline{\omega}_{k|N} - (\overline{v}_{k|N} - w_{y|N})\overline{\xi}_{k|N} + (u_{k|N} - w_{x|N})\overline{\omega}_{k|N} \\ +(v_{k|N} - w_{y|N})\overline{\xi}_{k|N} + (\overline{u}_{k|N} - w_{x|N})\omega_{k|N} + (\overline{v}_{k|N} - w_{y|N})\xi_{k|N}]\Delta t \end{bmatrix} \tag{23}$$

$$V_{\min} \le \frac{(\overline{u}_{k|N} - w_{x|N})(u_{k|N} - w_{x|N}) + (\overline{v}_{k|N} - w_{y|N})(v_{k|N} - w_{y|N})}{\sqrt{(\overline{u}_{k|N} - w_{x|N})^2 + (\overline{v}_{k|N} - w_{y|N})^2}} \tag{24}$$

$$(u_{k|N} - w_{x|N})^2 + (v_{k|N} - w_{y|N})^2 \le {V_{\max}}^2 \tag{25}$$

$$-g\tan\varphi_{\max} / V_{\max} \le \omega_{k|N} \le g\tan\varphi_{\max} / V_{\max} \tag{26}$$

$$-a_{\max} / V_{\max} \le \xi_{k|N} \le a_{\max} / V_{\max} \tag{27}$$

where $\overline{u}_{k|N}, \overline{v}_{k|N}, \overline{\omega}_{k|N}$, and $\overline{\xi}_{k|N}$ are the reference points for convexifications, and they are defined as the solutions of the previous MPC except that

$$[\overline{u}_{N+N_p|N} \;\; \overline{v}_{N+N_p|N} \;\; \overline{\omega}_{N+N_p-1|N} \;\; \overline{\xi}_{N+N_p-1|N}]^T = [\overline{u}_{N+N_p-1|N} \;\; \overline{v}_{N+N_p-1|N} \;\; 0 \;\; 0]^T$$

If the j-th neighboring aircraft's trajectory is also calculated by the MPC, $[x_k^{(j)} \;\; y_k^{(j)}]^T$ will approach $[\hat{x}_{k|N}^{(j)} \;\; \hat{y}_{k|N}^{(j)}]^T$ as close as possible. Nevertheless, Eq. (20) does not enforce $[x_k^{(j)} \;\; y_k^{(j)}]^T$ to be within $E(\hat{x}_{k|N}, \hat{y}_{k|N}, \boldsymbol{P}_{\text{pos},k|N}, \mu)$. Thus, as a result of the MPC optimization to improve other objective terms and/or constraints, or as a result of applying any other control law, $[x_k^{(j)} \;\; y_k^{(j)}]^T \notin E(\hat{x}_{k|N}, \hat{y}_{k|N}, \boldsymbol{P}_{\text{pos},k|N}, \mu)$ may occur and it may potentially cause conflict as well. To avoid this, we enforce the following two inequalities for separation instead of Eq. (20):

$$\frac{1}{\sqrt{(\hat{x}_{k|N}^{(0)} - \hat{x}_{k|N}^{(j)})^2 + (\hat{y}_{k|N}^{(0)} - \hat{y}_{k|N}^{(j)})^2}} \begin{bmatrix} \hat{x}_{k|N}^{(0)} - \hat{x}_{k|N}^{(j)} \\ \hat{y}_{k|N}^{(0)} - \hat{y}_{k|N}^{(j)} \end{bmatrix}^T \begin{bmatrix} x_{k|N} - (\hat{x}_{k|N}^{(0)} + \hat{x}_{k|N}^{(j)})/2 \\ y_{k|N} - (\hat{y}_{k|N}^{(0)} + \hat{y}_{k|N}^{(j)})/2 \end{bmatrix} \ge \frac{R}{2}(1 - d^{(j)}) \tag{28}$$

$$\frac{1}{\sqrt{(\hat{x}_{k|N}^{(0)} - \overline{x}_{k|N}^{(j)})^2 + (\hat{y}_{k|N}^{(0)} - \overline{y}_{k|N}^{(j)})^2}} \begin{bmatrix} \hat{x}_{k|N}^{(0)} - \overline{x}_{k|N}^{(j)} \\ \hat{y}_{k|N}^{(0)} - \overline{y}_{k|N}^{(j)} \end{bmatrix}^T \begin{bmatrix} x_{k|N} - \overline{x}_{k|N}^{(j)} \\ y_{k|N} - \overline{y}_{k|N}^{(j)} \end{bmatrix} \ge R(1 - d^{(j)}) \tag{29}$$

where $[\overline{x}_{k|N}^{(j)} \;\; \overline{y}_{k|N}^{(j)}]^T$ is the point in $E(\hat{x}_{k|N}^{(j)}, \hat{y}_{k|N}^{(j)}, \boldsymbol{P}_{\text{pos},k|N}^{(j)}, \mu)$ with the minimum Euclidian distance from $[\overline{x}_{k|N}^{(0)} \;\; \overline{y}_{k|N}^{(0)}]^T$, and $d^{(1)}, \cdots, d^{(M)}$ are the slack variables that are introduced to guarantee the solvability of the MPC problem at any situation. Figures 1 and 2 illustrates the geometric relationship between the uncertain region $E(\hat{x}_{k|N}, \hat{y}_{k|N}, \boldsymbol{P}_{\text{pos},k|N}, \mu)$ and the feasible region given by Eqs. (28) and (29). As far as Eq. (28) with $d^{(j)} = 0$ is satisfied, the conflict can be avoided even if each aircraft's trajectory is optimized in a decentralized manner. Similar approaches for decentralization as above were adopted in Refs. 26 and 27. To account for the trajectory uncertainty of neighboring aircraft to which the proposed MPC may not be applied, we further enforce Eq. (29). By penalizing nonzero $d^{(j)}$ in the objective function as follows, it is possible to obtain the solution which maximally maintains the separation

$$\hat{J} := J + \sum_{j=1}^{M} \overline{\rho}_4 d^{(j)} \tag{30}$$

where $\overline{\rho}_4$ is a sufficiently large weight.

Consequently, the resulting MPC problem is formulated as follows.

minimize : Eq. (30)
subject to: Eq. (22)
Eq. (23), $k = N, \cdots, N + N_p - 1$,
Eqs. (24) and (25), $k = N+1, \cdots, N + N_p$,
Eqs. (26) and (27), $k = N, \cdots, N + N_p - 1$, and
Eqs. (28) and (29), $k = N+1, \cdots, N + N_p$, $j = 1, \cdots, M$
decision variables: $[x_{k|N} \;\; y_{k|N} \;\; u_{k|N} \;\; v_{k|N}]^T$, $k = N, \cdots, N + N_p$, $[\omega_{k|N} \;\; \xi_{k|N}]^T$, $k = N, \cdots, N + N_p - 1$, $d^{(j)}$, $j = 1, \cdots, M$.

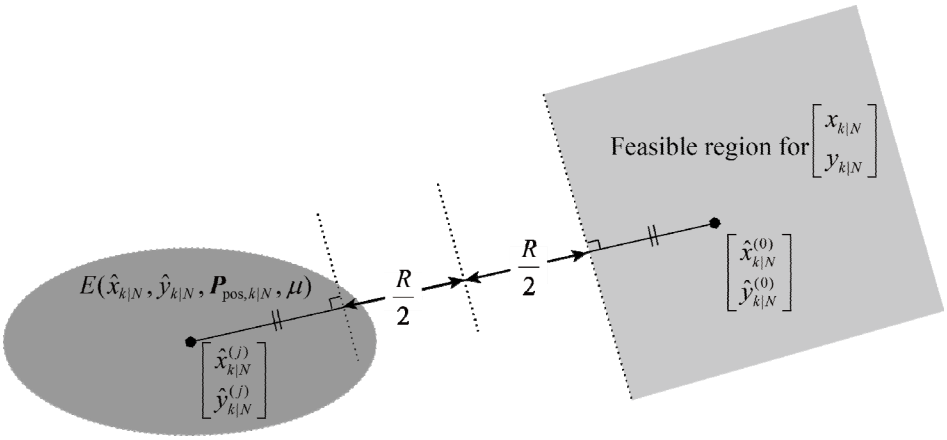

Figure 1. Ellipsoid representing the uncertainty of $[x_{k|N}^{(j)} \quad y_{k|N}^{(j)}]^T$ and the feasible region for decentralized optimization given by Eq. (28) with $d^{(j)} = 0$.

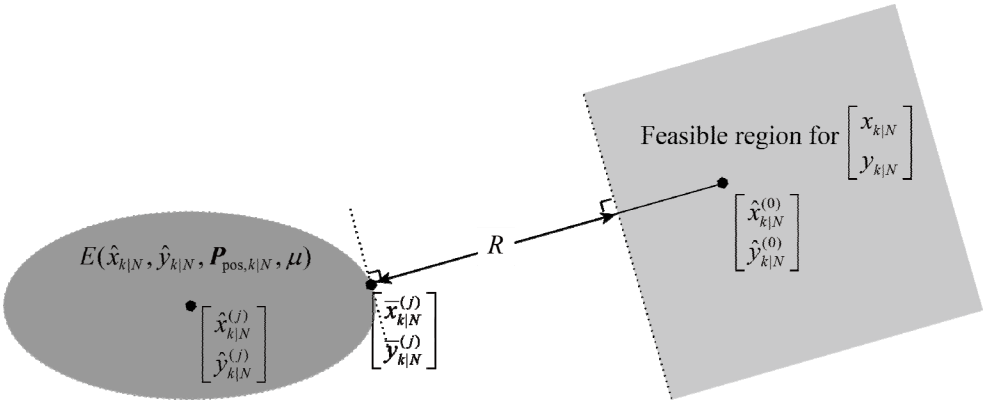

Figure 2. Ellipsoid representing the uncertainty of $[x_{k|N}^{(j)} \quad y_{k|N}^{(j)}]^T$ and the feasible region accounting for the uncertainty given by Eq. (29) with $d^{(j)} = 0$.

III. Numerical Examples

We show some numerical examples by applying the proposed method. Parameters used in the simulations are summarized in Table 1. The computer specifications used for the simulations are as follows:

- CPU: Intel® Xeon™ E5-2630 v4 2.2GHz (dual processor)
- RAM: 64.0GB
- OS: Windows 10 64-bit

As the solver for the convex QCQPs/QPs, we used an IBM® ILOG® CPLEX® 12.63

Table 1. Parameters for simulations.

Parameter	Value	Parameter	Value
$V_{\min}$ [km/s]	0.23	R [km]	9.26
$V_{\max}$ [km/s]	0.27	Δt [s]	2.0
$\varphi_{\max}$ [rad]	$\pi/6$	$N - N_I$	10
$a_{\min}$ [km/s^2]	-0.1g	N_p	40
$a_{\max}$ [km/s^2]	0.1g		

Firstly, we considered a scenario where two aircraft were initially in conflict under a constant wind condition. The initial position of aircraft A and B were specified as $(-43.2[\mathrm{km}], 0.0[\mathrm{km}])$ and $(31.5[\mathrm{km}], 31.5[\mathrm{km}])$, respectively, while their destination waypoints were specified as A : $(43.2[\mathrm{km}], 0.0[\mathrm{km}])$ and B : $(-31.5[\mathrm{km}], -31.5[\mathrm{km}])$. The wind vector were given as $[-0.02[\mathrm{km/s}] \ -0.02[\mathrm{km/s}]]^T$. For comparison, we considered the proposed method with and without intent inference. In the method without intent inference, the desirable velocity vector $[u_{dk} \ \ v_{dk}]^T$ was replaced by the current velocity vector, and no uncertainty of the predicted trajectory was considered, i.e., $\mu = 0$. In the method with intent inference, on the other hand, the parameters associated with the uncertainty were specified as follows:

$$\sigma_{wx} = \sigma_{wy} = 0.01[\mathrm{km/s}],$$
$$\sigma_{\omega} = 8.73 \times 10^{-3}[\mathrm{rad/s}],$$
$$\sigma_{a} = 1.96 \times 10^{-4}[\mathrm{km/s^2}],$$
$$\sigma_{\tau} = 0.1,$$
$$\sigma_{ud} = \sigma_{vd} = 0.02[\mathrm{km/s}],$$
$$\hat{\tau} = 4.0[\mathrm{s}], \quad c = 1.25, \quad \mu = 3.0$$

Figure 3 shows the trajectories in the case where only aircraft A had an intent to resolve the conflict. As can be seen in this figure, the trajectory of aircraft A by the method with intent inference were conservative in conflict resolution, because it predicted the uncertain trajectory. Thus, the distance between the aircraft at the closest point of approach (CPA) was 13.08[km], which was greater than the specified separation minimum of $R = 9.26[\mathrm{km}]$. It was also observed that the conflict resolution maneuver by the method with intent inference was initiated earlier than that without intent inference.

Figure 4 shows the trajectories in the case where both aircraft A and B had intent to resolve the conflict. The same tendency of trajectory conservativeness by the method with intent inference as in the previous case was observed. Nevertheless, the coordinated conflict-free trajectories were successfully obtained with and without intent inference. The distances between the aircraft at CPA were 14.43[km] in the case with intent inference and 9.26[km] in the case without intent inference. The inferred weights corresponding to individual intent for this bilateral simulation are shown in Fig. 5. The intent of "conflict resolution" was dominant approximately from $t \in [76[\mathrm{s}], 138[\mathrm{s}]]$ for aircraft A and $t \in [80[\mathrm{s}], 84[\mathrm{s}]]$, $t \in [104[\mathrm{s}], 138[\mathrm{s}]]$ for aircraft B. These results are consistent with the conflict resolution maneuvers in the trajectories.

We also considered a scenario where aircraft B executed maneuvers but had no actual intent of conflict resolution, hence only aircraft A needed to resolve conflict. The initial position of aircraft A and B were specified as $(-49.5[\mathrm{km}], 0.0[\mathrm{km}])$ and $(0.0[\mathrm{km}], 40.0[\mathrm{km}])$, respectively. The destination waypoint for aircraft A was specified as A : $(40.0[\mathrm{km}], 0.0[\mathrm{km}])$, and two destination waypoints B1 : $(0.0[\mathrm{km}], 6.75[\mathrm{km}])$ and B2: $(-40.0[\mathrm{km}], 0.0[\mathrm{km}])$ were assigned to aircraft B. No wind was simulated in this scenario.

The trajectories with and without intent inference in this scenario were shown in Fig. 6. While the distance between the aircraft at CPA for the case without intent inference was 6.94[km], that for the case with intent inference was 9.08[km], that was almost equal to the specified value of $R = 9.26[\mathrm{km}]$. This result indicates the possible advantage of applying the intent inference with trajectory uncertainty for conflict resolution. Figure 7 shows the time histories of the inferred weights corresponding to individual intent. As can be seen in this figure, the intent of "conflict resolution" in aircraft B became dominant soon after it passed waypoint B1. Although aircraft B had no actual intent of conflict resolution, the maneuver of aircraft B resulted in assisting to resolve the conflict in accord with the intentional maneuver by aircraft A.

In each simulations, we also measured the computational time of the proposed method per sampling period, i.e., the sum of the computational times for the intent inference, the trajectory prediction, and the MPC, per sampling period, and it was 0.17[s] in the worst case. Since this value is much less than the specified sampling period $\Delta t = 2.0[\mathrm{s}]$, we can confirm the real-time applicability of the proposed method.

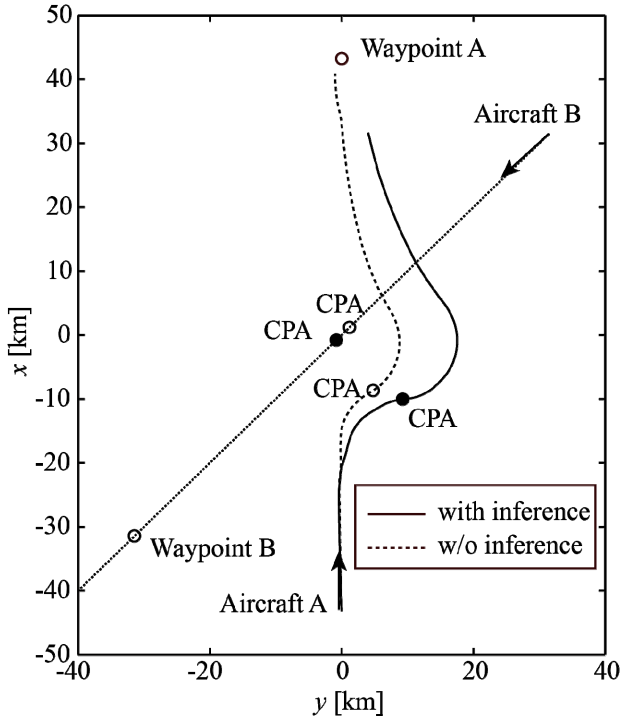

Figure 3. Trajectories of unilateral conflict resolution, where aircraft B flies straight.

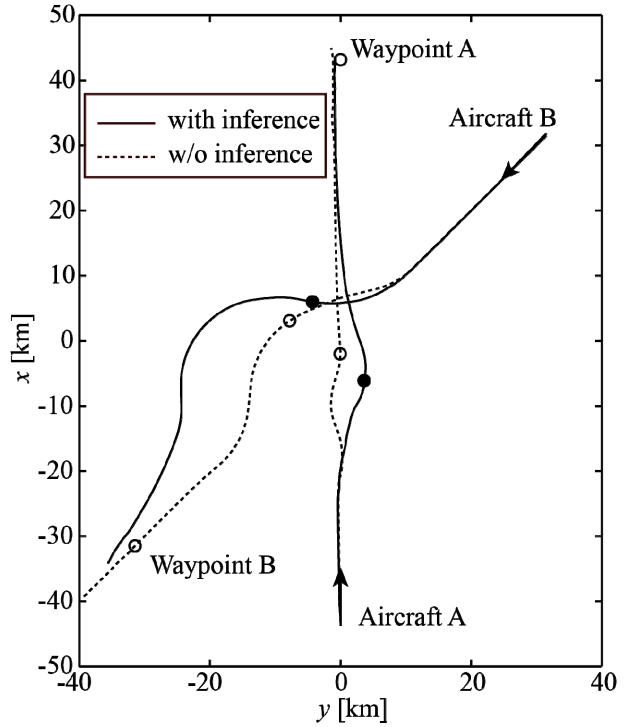

Figure 4. Trajectories of bilateral conflict resolutions.

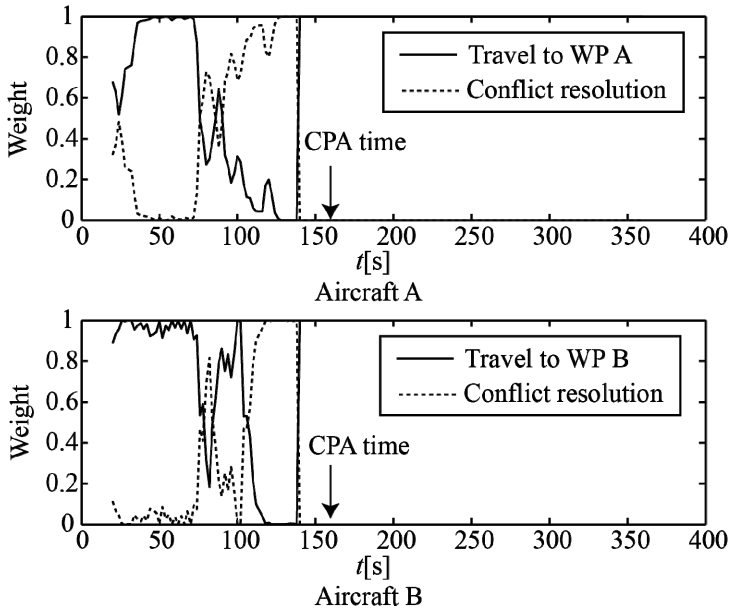

Figure 5. Time history of the intent inferred by the trajectories in Figure 4.

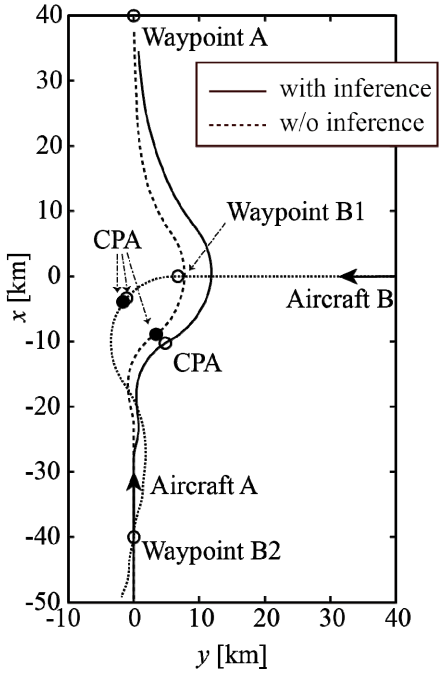

Figure 6. Trajectories of unilateral conflict resolution, where aircraft B executes maneuver without intent of conflict resolution

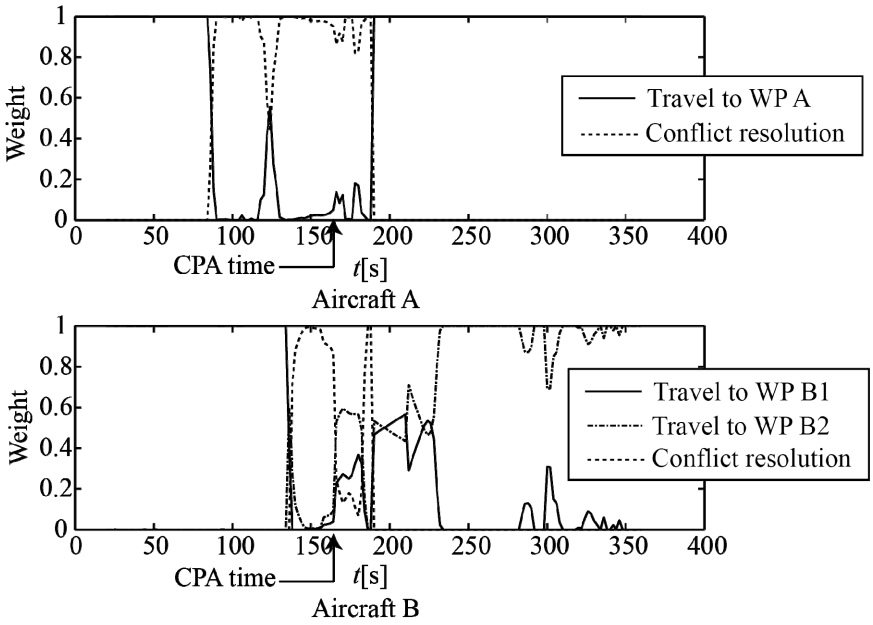

Figure 7. Time history of the intent inferred by the trajectories in Figure 6.

IV. Conclusions

This paper proposed a decentralized model predictive control (MPC) for conflict detection and resolution using intent-based probabilistic trajectory prediction combined with intent inference. By incorporating the inverse optimal control for intent inference and the unscented transform for the prediction of nonlinear state propagation, the method can cover the linear/nonlinear uncertain behaviors of the aircraft due to the wind effect, the deviation of navigation strategy, and the inaccuracy of inferred intent. Through numerical simulations, the effectiveness of the method was demonstrated in terms of the validity of the obtained conflict-free trajectories and the computational efficiency.

Future work includes, but is not limited to, the extension of the method to three-dimensional space and the inclusion of other flight intent such as avoiding a region and circling around a waypoint.

Appendix: Inverse Optimal Control for Intent Inference[12]

A. 1 Modeling of Motion and Flight Intent

Similarly to the conflict detection/resolution in the proposed method, we discretize the following system

$$\begin{bmatrix} \dot{x} \\ \dot{y} \\ \dot{u} \\ \dot{v} \\ \dot{\omega} \end{bmatrix} = \begin{bmatrix} u \\ v \\ -(v-w_y)\omega + (u-w_x)\xi \\ (u-w_x)\omega + (v-w_y)\xi \\ \chi \end{bmatrix} \tag{31}$$

Let us denote the state and control input as $\boldsymbol{x}_k := [x_k \quad y_k \quad u_k \quad v_k \quad \omega_k]^T$ and $\boldsymbol{u}_k := [\xi_k \quad \chi_k]^T$, respectively. To define the objective function of the "target" neighboring aircraft, we introduce measures of the ideal heading for individual flight intent, as follows.

Let $(x_r^{(n)}, y_r^{(n)})$, $n = 1, \cdots, N_w$, be the position of the n-th waypoint, and let $\boldsymbol{\theta}_{n,k}$ be the deviation of the current heading from the line-of-sight direction of $(x_r^{(n)}, y_r^{(n)})$, i.e.,

$$\boldsymbol{\theta}_{n,k} := \frac{1}{\sqrt{u_k^2 + v_k^2}} \begin{bmatrix} u_k \\ v_k \end{bmatrix} - \frac{1}{\sqrt{(x_r^{(n)} - x_k)^2 + (y_r^{(n)} - y_k)^2}} \begin{bmatrix} x_r^{(n)} - x_k \\ y_r^{(n)} - y_k \end{bmatrix} \tag{32}$$

Then, the flight intent of direct travel to $(x_r^{(n)}, y_r^{(n)})$ can be formulated as the minimization of $\sum_k \boldsymbol{\theta}_{n,k}{}^T \boldsymbol{\theta}_{n,k}$.

In order to account for the intent to resolve conflict with a neighboring aircraft, we assume that the pilot/operator/autopilot proactively attempts to ensure that the predicted closest distance between the target aircraft and any neighboring aircraft is larger than R. Let us define the relative vectors as follows:

$$\boldsymbol{z}_{i,k} := \begin{bmatrix} x_k - \hat{x}_{i,k} \\ y_k - \hat{y}_{i,k} \end{bmatrix}, \quad \boldsymbol{w}_{i,k} := \begin{bmatrix} u_k - \hat{u}_{i,k} \\ v_k - \hat{v}_{i,k} \end{bmatrix}$$

where $(\hat{x}_{i,k}, \hat{y}_{i,k})$ and $(\hat{u}_{i,k}, \hat{v}_{i,k})$ are the position and the ground velocity of the i-th $(i = 1, \cdots, L)$ neighboring aircraft at time $t = k\Delta t$. The intent to resolve conflict can then be modeled as the intent to make the current heading as close as possible to the ideal direction for conflict resolution, where the ideal direction to the right (denoted as $\boldsymbol{d}_{i,k}^+$) or to the left (denoted as $\boldsymbol{d}_{i,k}^-$) is measured in the relative coordinate system (see Fig. 8), i.e., it is modeled as $\sum_k \min[(\boldsymbol{\eta}_{i,k}^+)^T \boldsymbol{\eta}_{i,k}^+, (\boldsymbol{\eta}_{i,k}^-)^T \boldsymbol{\eta}_{i,k}^-]$, where

$$\boldsymbol{\eta}_{i,k}^+ := \frac{\boldsymbol{w}_{i,k}}{|\boldsymbol{w}_{i,k}|} - \begin{bmatrix} \sqrt{\max(0, \boldsymbol{z}_{i,k}{}^T \boldsymbol{z}_{i,k} - R^2)} & -R \\ R & \sqrt{\max(0, \boldsymbol{z}_{i,k}{}^T \boldsymbol{z}_{i,k} - R^2)} \end{bmatrix} \frac{(-\boldsymbol{z}_{i,k})}{|\boldsymbol{z}_{i,k}|^2}$$

$$\boldsymbol{\eta}_{i,k}^- := \frac{\boldsymbol{w}_{i,k}}{|\boldsymbol{w}_{i,k}|} - \begin{bmatrix} \sqrt{\max(0, \boldsymbol{z}_{i,k}{}^T \boldsymbol{z}_{i,k} - R^2)} & R \\ -R & \sqrt{\max(0, \boldsymbol{z}_{i,k}{}^T \boldsymbol{z}_{i,k} - R^2)} \end{bmatrix} \frac{(-\boldsymbol{z}_{i,k})}{|\boldsymbol{z}_{i,k}|^2}$$

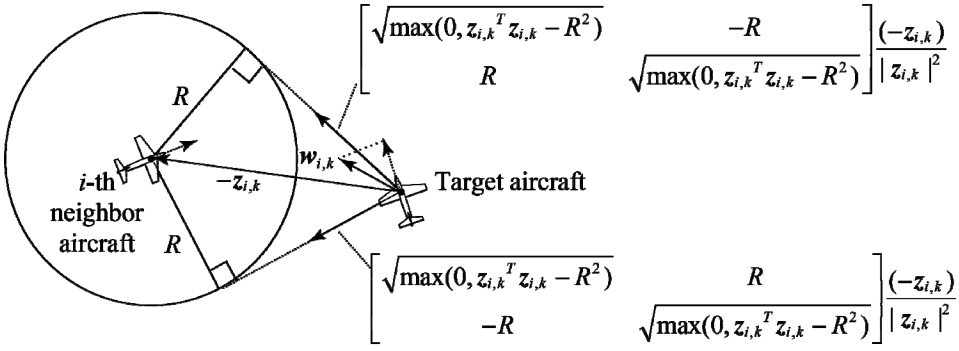

Figure 8. Ideal heading vector for conflict resolution in the relative coordinate system.

A.2. Forward Optimal Control Problem and Optimality Condition

For the above model, we can state the discrete-time optimal control problem defined over the finite time horizon $[N_I \Delta t, N\Delta t]$ $(N > N_I)$, as follows:

$$\underset{\boldsymbol{x}_{NI}, \boldsymbol{u}_{NI}, \cdots, \boldsymbol{x}_N, \boldsymbol{u}_N}{\text{minimize}}$$

$$J_N := \sum_{k=N_I+1}^{N} \sum_{n=1}^{N_w} \{q_{n|N} (\boldsymbol{\theta}_{n,k})^T \boldsymbol{\theta}_{n,k} + \sum_{k=N_I+1}^{N} \sum_{i=1}^{L} s_{i|N} \min\{(\boldsymbol{\eta}_{i,k}^+)^T \boldsymbol{\eta}_{i,k}^+, \ (\boldsymbol{\eta}_{i,k}^-)^T \boldsymbol{\eta}_{i,k}^-\} + \sum_{k=N_I}^{N} (r_{1|N} \xi_k{}^2 + r_{2|N} \chi_k{}^2) \tag{33}$$

subject to

$$\boldsymbol{c}_k := \boldsymbol{x}_k - \boldsymbol{x}_{k-1} - \frac{\Delta t}{2}[\boldsymbol{f}(\boldsymbol{x}_k, \boldsymbol{u}_k) + \boldsymbol{f}(\boldsymbol{x}_{k-1}, \boldsymbol{u}_{k-1})] = \boldsymbol{0}, \quad k = N_I + 1, \cdots, N \tag{34}$$

$$\boldsymbol{c}_{N_I} := \boldsymbol{x}_{N_I} - \tilde{\boldsymbol{x}}_{N_I} = \boldsymbol{0} \tag{35}$$

where $q_{1|N}, \cdots, q_{N_w|N}$, $s_{1|N}, \cdots, s_{L|N}$ are nonnegative weights, $r_{1|N}$ and $r_{2|N}$ are positive weights, $\tilde{\boldsymbol{x}}_{N_I}$ is the actual state of the aircraft at time $t = N_I \Delta t$, and $\boldsymbol{f}(\boldsymbol{x}_k, \boldsymbol{u}_k)$ is defined as

$$\boldsymbol{f}(\boldsymbol{x}_k, \boldsymbol{u}_k) := \begin{bmatrix} u_k \\ v_k \\ (u_k - w_{xk})\xi_k - (v_k - w_{yk})\omega_k \\ (v_k - w_{yk})\xi_k + (u_k - w_{xk})\omega_k \\ \chi_k \end{bmatrix}$$

Equation (34) can be derived by applying the modified Euler method to Eq. (31). The minimization of the quadratic terms in ξ_k and χ_k in Eq. (33) represents the intent of maintaining the airspeed V and the rate of turn ω, respectively.

Let the Lagrange multipliers corresponding to the equality constraints of Eqs. (34) and (35) be $\boldsymbol{\lambda}_{k|N}$ $(k = N_I + 1, \cdots, N)$ and $\boldsymbol{\lambda}_{N_I|N}$, respectively. Then, the second-order sufficient conditions for local optimality of the solution to the forward optimal control problem given by Eqs. (33)−(35) are as follows:

- The primal feasibility, as stated by Eqs. (34) and (35),
- The dual feasibility, i.e.,

$$\nabla J_N - \boldsymbol{\lambda}_{N_I|N}{}^T \nabla \boldsymbol{x}_M - \sum_{k=N_I+1}^{N} \boldsymbol{\lambda}_{k|N}{}^T \left[\nabla \boldsymbol{x}_k - \nabla \boldsymbol{x}_{k-1} - \frac{\Delta t}{2} \{ \nabla \boldsymbol{f}(\boldsymbol{x}_k, \boldsymbol{u}_k) + \nabla \boldsymbol{f}(\boldsymbol{x}_{k-1}, \boldsymbol{u}_{k-1}) \} \right] = \boldsymbol{0} \tag{36}$$

- The positive definiteness of the projected Hessian of the Lagrangian[27], i.e.,

$$\boldsymbol{Z}_N{}^T \boldsymbol{H}_N \boldsymbol{Z}_N \succ \boldsymbol{0} \tag{37}$$

where

$$\boldsymbol{H}_N := \nabla^2 J_N + \frac{\Delta t}{2} \sum_{k=N_I+1}^{N} \boldsymbol{\lambda}_{k|N}{}^T [\nabla^2 \boldsymbol{f}(\boldsymbol{x}_k, \boldsymbol{u}_k) + \nabla^2 \boldsymbol{f}(\boldsymbol{x}_{k-1}, \boldsymbol{u}_{k-1})] \tag{38}$$

and $\boldsymbol{Z}_N \in \mathbb{R}^{7(N-N_I+1)\times 2(N-N_I+1)}$ is a matrix whose column vectors are the approximated bases of the null space of the gradient matrix $[\nabla \boldsymbol{c}_{N_I} \;\; \nabla \boldsymbol{c}_{N_I+1} \;\; \cdots \;\; \nabla \boldsymbol{c}_N]$. We adopt approximate matrix of $\boldsymbol{Z}_N$ so that $\boldsymbol{Z}_N{}^T \boldsymbol{H}_N \boldsymbol{Z}_N$ becomes block diagonal matrix.

A.3. Inverse Optimal Control Problem for Intent Inference

For notational simplicity, we concatenate the weight of the objective function and the Lagrange multiplier as follows:

$$\boldsymbol{\rho}_N := [q_{1|N} \;\; \cdots \;\; q_{N_w|N} \;\; s_{1|N} \;\; \cdots \;\; s_{L|N} \;\; r_{1|N} \;\; r_{2|N}]^T \in \mathbb{R}^{N_\rho}$$
$$\boldsymbol{\lambda}_N := [\boldsymbol{\lambda}_{N_I|N}{}^T \;\; \cdots \;\; \boldsymbol{\lambda}_{N|N}{}^T]^T \in \mathbb{R}^{5(N-N_I+1)}$$

where $N_\rho = N_w + L + 2$. Assume that the time history of the target aircraft's state and control input, the neighboring aircraft's position and velocity, and the wind velocity over the time domain $[N_I \Delta t, N\Delta t]$ are given at time $t = N\Delta t$. Moreover, we assume that the given history of the target aircraft is an approximately optimal solution to the forward optimal control problem of Eqs. (33)−(35), that is, in the least-squares sense, $\{\boldsymbol{x}_{N_I}, \boldsymbol{u}_{N_I}, \cdots, \boldsymbol{x}_N, \boldsymbol{u}_N\}$ satisfies the optimality conditions given by Eqs. (34)−(37).

The inverse optimal control problem over the finite horizon $[N_I \Delta t, N\Delta t]$ can then be stated as follows:

$$\underset{\boldsymbol{\rho}_N, \boldsymbol{\lambda}_N}{\text{minimize}}: \left\| \nabla J_N - \boldsymbol{\lambda}_{N_I|N}{}^T \nabla \boldsymbol{x}_{N_I} - \sum_{k=N_I+1}^{N} \boldsymbol{\lambda}_{k|N}{}^T \left[\nabla \boldsymbol{x}_k - \nabla \boldsymbol{x}_{k-1} - \frac{\Delta t}{2} \{ \nabla \boldsymbol{f}(\boldsymbol{x}_k, \boldsymbol{u}_k) + \nabla \boldsymbol{f}(\boldsymbol{x}_{k-1}, \boldsymbol{u}_{k-1}) \} \right] \right\|^2 + \hat{\sigma} \left\| \boldsymbol{\rho}_N - \boldsymbol{\rho}_{N-1} \right\|^2 \tag{39}$$

subject to:

$$\sum_{n=1}^{N_w} q_{n|N} + \sum_{i=1}^{L} s_{i|N} = 1 \tag{40}$$

$$\boldsymbol{\rho}_N \geq \begin{bmatrix} \boldsymbol{0}_{(N_\rho - 2)\times 1} \\ \varepsilon_0 \\ \varepsilon_0 \end{bmatrix} \tag{41}$$

$$\left.\begin{aligned} h_{k,11} &\geq |\, h_{k,12} \,| + \varepsilon_0 \\ h_{k,22} &\geq |\, h_{k,12} \,| + \varepsilon_0 \end{aligned}\right\}, \quad k = 1, \cdots, N - N_I + 1 \tag{42}$$

where $\begin{bmatrix} h_{k,11} & h_{k,12} \\ h_{k,12} & h_{k,22} \end{bmatrix}$ is a k-th block diagonal submatrix of $\boldsymbol{Z}_N{}^T \boldsymbol{H}_N \boldsymbol{Z}_N$, $\hat{\sigma}$ is a positive constant, and ε_0 is a small positive constant.

For uniqueness of the inferred solution, the second term in Eq. (39) and the dehomogenization condition in the form of Eq. (40) is added. The problem given by Eqs. (39)-(42) is a convex QP which has sparse patterns in the Jacobian of the inequality constraints and the Hessian of the Lagrangian. Thus, it can be computed rapidly using an off-the-shelf solver.

After solving the inverse optimal control problem, the intent corresponding to the largest weight is chosen as the "inferred intent." Then, the direction (u_{dk}, v_{dk}) is specified as the ideal direction to attain the inferred intent such that $\boldsymbol{\theta}_{n,k} = \mathbf{0}$ holds if the inferred intent is to direct travel to a WP or $\min\{(\boldsymbol{\eta}_{i,k}^{+})^T \boldsymbol{\eta}_{i,k}^{+}, (\boldsymbol{\eta}_{i,k}^{-})^T \boldsymbol{\eta}_{i,k}^{-}\} = \mathbf{0}$ holds if the inferred intent is to resolve conflict with a neighboring aircraft.

Acknowledgments

This research was supported by JSPS KAKENHI Grant Number JP15K18289.

References

[1]"Concept of Operations for the Next Generation Air Transportation System Ver. 3.2," Federal Aviation Administration, Joint Planning, and Development Office, 2010.

[2]"European ATM Master Plan Edition 2," Single European Sky ATM Research Joint Undertaking, Brussels, 2012.

[3]"Long-Term Vision for the Future Air Traffic Systems," Ministry of Land, Infrastructure, Transport, and Tourism Study Group for the Future Air Traffic Systems, Tokyo, 2010.

[4]R. S. Committee-186, "Minimum Aviation System Performance Standards for Automatic Dependent Surveillance Broadcast (ADS-B)," RTCA, RTCA/D0-242, 1998.

[5]Barhydt, R. and Warren, A., "Newly Enacted Intent Changes to ADS-B MASPS: Emphasis on Operations, Compatibility, and Integrity," *Proceedings of AIAA Guidance, Navigation, and Control Conference*, Monterey, CA, AIAA 2002-4932, 2002.

[6]Ramasamy, S., Sabatini, R., Gardi, A. G. and Liu, Y., "Novel Flight Management System for Real-time 4-Dimensional Trajectory Based Operations," *Proceedings of AIAA Guidance, Navigation, and Control Conference*, Boston, MA, AIAA 2013-4763, 2013.

[7]Reynolds, T. and Hansman, R., "Conformance Monitoring Approaches in Current and Future Control Environments," *Proceedings of 19th IEEE/AIAA Digital Avionics Systems Conference*, Irvine, CA, 2002.

[8]Krozel, J. and Andrisani, D., "Intelligent Path Prediction for Vehicular Travel," IEEE Transactions on Systems, Man, and Cybernetics, Vol. 23, 1993, pp.478-487.

[9]Krozel, J.,and, D. and Andrisani, D, "Intent Inference with Path Prediction," *Journal of Guidance, Control, and Dynamics*, Vol. 29, No. 2, 2006, pp. 225-236.

[10]Yepes, J. L., Hwang, I. and Rotea, M., "New Algorithms for Aircraft Intent Inference and Trajectory Optimization," *Journal of Guidance, Control, and Dynamics*, Vol. 30, No. 2, 2007, pp. 370-382.

[11]Yokoyama, N., "Inference of Flight Mode of Aircraft Including Conflict Resolution," *Proceedings of 2016 American Control Conference*, Boston, MA, 2016, pp. 6729-6734.

[12]Yokoyama, N., "Inference of Aircraft Intent via Inverse Optimal Control Including Second-Order Optimality Condition," *Journal of Guidance, Control, and Dynamics*, accepted for publication.

[13]Kuchar, J. and Yang, L., "A Review of Conflict Detection and Resolution Modeling Methods," *IEEE Transactions on Intelligent Transportation Systems*, Vol. 1, No. 4, pp. 178-189, 2000.

[14]Zhao, Y. and Zheng, Q. M., "Modeling Uncertainties in Intents, Guidance, and Pilot Actions for Advanced Trajectory Synthesis," *Proceedings of 12th AIAA Aviation, Technology, Integration and Operations Conference*, Indianapolis, IN, U.S.A., AIAA 2012-5421, 2012.

[15]Paielli, R. and Erzberger, H., "Conflict Probability Estimation for Free Flight," *Journal of Guidance, Control, and Dynamics*, Vol. 20, No. 2, 1997, pp. 232-238.

[16]Hwang I. and Seah, C. E., "Intent-Based Probabilistic Conflict Detection for the Next Generation Air Transportation System," *Proceedings of the IEEE*, Vol. 96, No. 12, 2008, pp. 2040-2059.

[17]Liu, W. and Hwang, I., "Probabilistic Trajectory Prediction and Conflict Detection for Air Traffic Control," *Journal of Guidance, Control, and Dynamics*, Vol. 34, No. 6, pp. 1779-1789, 2011.

[18]Matsuno, Y., Tsuchiya, T., and Matayoshi, N., "Near-Optimal Control for Aircraft Conflict Resolution in the

Presence of Uncertainty," *Journal of Guidance, Control, and Dynamics*, Vol. 39, No. 2, 2016, pp. 326-338.
[19]Xiu, D. and Karniadakis, G. E., "The Wiener-Askey Polynomial Chaos for Stochastic Differential Equations, *SIAM Journal on Scientific Computing,* Vol. 24, No. 2, 2002, pp.619-644.
[20]Julier, S., Uhlmann, J., and Durrant-Whyte, H. F., "A New Method for the Nonlinear Transformation of Means and Covariances in Filters and Estimators," IEEE Transactions on Automatic Control, Vol. 45, No. 3, 2000, pp. 477-482.
[21]Julier, S. and Uhlmann, J. K., "Unscented Filtering for Nonlinear Estimation," Proceedings of the IEEE, Vol. 92, No. 3, 2004, pp. 401-422.
[22]Ross M., Proulx, R., and Karpenko, Mark, "Unscented Optimal Control for Orbital and Proximity Operations in an Uncertain Environment: A New Zermelo Problem," *Proceedings of AIAA/AAS Astrodynamics Specialist Conference*, AIAA SPACE Forum, San Diego, CA, AIAA 2014-4423, 2014.
[23]Dinh, Q. T., Savorgnan, C, and Diehl, M., "Adjoint-Based Predictor-Corrector Sequential Convex Programming for Parametric Nonlinear Optimization," *SIAM Journal on Optimization*, Vol. 22, No. 4, pp. 1258-1284, 2012.
[24]Boyd, S. and Vandenberghe, L., *Convex Optimization*, Cambridge University Press, Cambridge, U. K., 2004.
[25]Yokoyama, N., "Model Predictive Control for Parallel Planning of Conflict-Free Trajectories for Multiple Aircraft," *Transactions of the Japan Society for Aeronautical and Space Sciences*, Vol. 57, No. 6, 2014, pp. 352-360.
[26]Yokoyama, N., "Decentralized Model Predictive Control for Planning Three-Dimensional Conflict-Free Trajectories," *Proceedings of the AIAA Guidance, Navigation, and Control Conference, AIAA SciTech Forum*, National Harbor, MD, AIAA 2014-0970, 2014.
[27]Gill, P. E., Murray, W. and Margaret, H. W., *Practical Optimization*, Elsevier, Oxford, U.K., 1986, pp. 77-82.